

SAFT-P: A Plaquette-Level Perturbation for Self-Assembly in Patchy Colloids

Hamza Çoban^{1,*} and Alfredo Alexander-Katz^{2,†}

¹*Department of Physics, Massachusetts Institute of Technology, Cambridge, Massachusetts 02139, United States*

²*Department of Materials Science and Engineering,
Massachusetts Institute of Technology, Cambridge, Massachusetts 02139, United States*

(Dated: March 9, 2026)

We introduce SAFT-P, a plaquette-level extension of Statistical Associating Fluid Theory for patchy particles. By treating local clusters as associating superparticles and contracting their free energy back to monomer densities, SAFT-P retains information about patch topology that is lost in conventional SAFT. Grand-canonical Monte Carlo simulations of binary and ternary mixtures show that SAFT-P captures topology-dependent critical points and coexistence curves and discriminates between particles with identical valence but different patch layouts. Beyond topology, incorporating plaquette-scale correlations also improves predictions in regimes where patch specific interactions are absent. Results indicate that resolving correlations at the plaquette scale provides an analytical route to model complex condensates and self-assembly with topology-sensitive local structure.

Multivalent macromolecules and patchy particles with directional binding can undergo liquid–liquid phase separation and self-organize into (biomolecular) condensates or colloidal networks whose rheology and connectivity are governed by binding valence, specificity, and orientation constraints.[1–5]. In biological settings, this idea is supported by cellular examples where multivalency drives phase transitions and enables switch-like control of signaling and organization [6, 7]. At the level of coarse-grained statistical mechanics, a central message from the patchy-particle literature is that valence alone is not sufficient: interaction specificity, steric constraints, conformation changes and patch placement bias, thereby shifting coexistence boundaries and the onset of aggregation or gelation [8–10]. Recent imaging studies further reveal heterogeneous network architectures within biomolecular condensates, consistent with nonuniform local connectivity and packing that emerge from directional and multivalent interactions [11].

In effectively two-dimensional environments, such as membrane-bound or surface-tethered systems, reduced coordination number and strong excluded-volume effects make local bonding geometry and patch arrangement particularly important in determining connectivity and phase behavior.[12–14]. Indeed, membrane- or surface-associated condensates provide concrete realizations of effectively two-dimensional phase separation in signaling contexts, where stoichiometry and local connectivity regulate both composition and function [15, 16]. Taken together, these studies motivate theoretical approaches that can distinguish particles or macromolecules with identical valence but different bonding geometry, since such differences can control the preferred local motifs and, consequently, the global phase behavior [4, 9].

This sensitivity to microscopic bonding rules has motivated sustained efforts to develop tractable theories across scales, from mean-field mixtures to network-based and field-theoretic descriptions. To model interaction networks and reproduce the equilibrium phase behavior

of biomolecular condensates, a range of frameworks have been developed across multiple coarse-graining levels and resolutions [17–19]. Mean-field descriptions of multicomponent liquids, such as Flory–Huggins-type models, provide a baseline and yield qualitative—and in some settings semi-quantitative—predictions for phase diagrams and multiphase coexistence [20–22]. Continuum phase-field (Cahn–Hilliard-type) approaches extend these free-energy descriptions to spatiotemporal dynamics, including binodal/spinodal evolution and coarsening, and can incorporate hydrodynamic effects to examine coarsening laws and pattern selection [23]. A sticker-and-spacer (or linker) framework, represents molecules as collections of binding sites connected by flexible segments and can capture sequence-encoded multivalency, percolation/gelation, and coupling between network formation and demixing; within this viewpoint, Flory–Stockmayer (FS) theory offers predictions for gelation thresholds and cluster-size statistics in step-growth/associative networks [24, 25]. Within the stickers-and-spacers paradigm, while some treatments emphasize effectively irreversible network growth, the Rubinstein–Semenov theory of associating polymers provides an analytical description of reversible network formation [26].

Coarse-grained “patchy-particle” models provide a minimalist route to encode multivalency and directional bonding. Developed on Wertheim’s thermodynamic perturbation theory (TPT), Statistical Associating Fluid Theory (SAFT) provides an analytical framework that has seen tremendous success as a molecularly grounded equation-of-state for associating fluids across diverse applications, including electrolyte solutions, polymer fluids, surfactant systems, supercritical fluids, and hydrogen-bonding liquids [27]. Building on this foundation, SAFT has also been proven successful in various applications in patchy colloids [4, 10, 28] and biomolecular condensates [29]. This framework is effective since it encodes valence and binding topology explicitly, allowing quantitative predictions of multi-phase coexistence, rigorous

assessment of how multivalency and sticker patterning shift phase boundaries, and rational design of interaction motifs to engineer condensate behavior [30, 31].

SAFT provides a molecular theory for associating fluids and has been widely used for quantitative predictions of equilibrium properties. Higher-order extensions (TPT2, TPT3) are available [32–34], and multibody/cluster-based corrections have been introduced to extend SAFT beyond the independent-site assumptions of TPT1—for example to treat arbitrary bonding-site geometries and situations where association involves strong multibody correlations [9]. Yet standard SAFT treatments remain insensitive to the spatial arrangement of bonding sites at fixed valence [35, 36] even though, that arrangement can be altered by geometric stereochemistry, e.g. cis/trans isomers or enantiomers, which changes which bonds can form simultaneously and which local motifs are accessible, thereby shifting assembly pathways and phase behavior [37, 38]. Ring corrections which depend on Monte Carlo integration have been proposed [39, 40], but they are not universal: they depend on the assumed bonding topology and site model, typically restricting the theory to a small subset of associating site pairs, fixed valence and geometry, and a limited class of cyclic graphs (frequently only small rings or cyclic dimers/double-bond motifs), rather than providing an unrestricted treatment of multicomponent plaquettes of arbitrary composition.

In this Letter, we introduce SAFT-P, an extension of SAFT that computes equilibrium properties at the cluster level to capture phase behavior in monomeric patchy-particle fluids. While the SAFT-P construction is general and can be formulated for other cluster choices and dimensions, here we use 2×2 plaquettes on a two-dimensional square lattice as the minimal cluster that resolves patch geometry and local packing constraints. Our approach provides a general treatment of 2D biomolecular condensates and protein mixtures, with sufficient resolution to capture spatial patch constraints. Across a set of binary and ternary mixtures, SAFT-P yields phase diagrams that are in closer agreement with simulation than conventional SAFT. Moreover, because SAFT-P resolves local patch geometry, it predicts phase separation between isomers, an effect that standard SAFT cannot capture.

Beyond mean-field treatments, SAFT offers a perturbative correction by systematically incorporating short-range correlations and directional bonding through a graph-theoretic cluster expansion [34, 41, 42]. Explicitly accounting for directional bonding, the first-order residual Helmholtz free energy due to association is given by:

$$\beta a_{\text{res}} = \left(\ln x - x + \frac{1}{2} \right), \quad x = \frac{\rho_0}{\rho}, \quad (1)$$

where x is the fraction of unbounded (monomer) species.

This formalism explicitly distinguishes monomer contributions from bonded species and provides a robust approach to model fluids with directional interactions.

In a generic many-component system, each particle has some fixed number of patches through which specific bonds occur. An isotropic interaction energy arises between any pair of neighbors regardless of the orientations of the patches. The free energy density per site of such a system can be written as the sum of the ideal entropic contribution and directional/anisotropic interaction terms. Here, we do not introduce empty sites since we add a non-interacting solvent as a different species in our framework and we assume the whole system is incompressible.

$$f = \sum_i \phi_i \ln \phi_i + \sum_i \phi_i \sum_s \left(\ln X_i^s - \frac{X_i^s}{2} + \frac{1}{2} \right), \quad (2)$$

where ϕ is the total particle fraction in a lattice, and ϕ_i the fraction of species i , X_i^s is the unbounded fraction of type s patches on type i component. The first term is the entropic term and the latter is due to directional patch bondings noting that nondirectional interactions may be embedded into directional setting. The fractions X_i^s forms a coupled equation system which generally does not have a closed-form solution

$$X_i^s = \left(1 + \sum_j \phi_j \sum_{s'} m_j^{s'} X_j^{s'} \Delta^{ss'} \right)^{-1}, \quad (3)$$

where the first sum is over all unique particle types and the second sum is over unique patches on type j particles. The number of type s patches on a type j molecule is given with $m_j^{s'}$. Lastly, $\Delta^{ss'}$ is the association strength of patches s and s' . For the lattice setting, it has a simpler expression, namely, $z \Delta^{ss'} = e^{\beta \epsilon_{ss'}} - 1$, where $\epsilon_{ss'}$ is the bonding energy between the patches. The extension to the continuum is straightforward: the lattice-specific $\Delta^{ss'}$ is replaced by the corresponding association integral for off-lattice patchy spheres [41, 43].

To capture condensation substructures and distinguish patchy particles that share the same valence but differ in patch arrangement, we use a plaquette-level coarse graining. We model small clusters of monomers as superparticles by mapping each (2×2) lattice plaquette—containing four primitive monomers—onto an effective particle with four superpatches. Each superpatch comprises two colocalized patches on the same plaquette edge and exhibits cooperative bonding: the two patches are treated as binding (or unbinding) simultaneously. To avoid double counting while retaining geometric resolution, we partition plaquette microstates into equivalence classes defined by their outgoing edge pattern (i.e., the set of external patches presented to neighboring plaquettes).

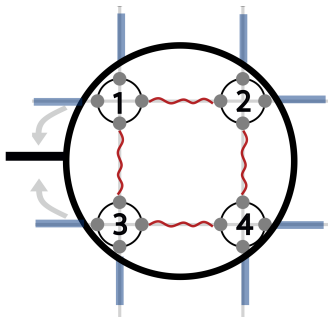


FIG. 1. A schematic of a 2×2 plaquette and conversion of it into a superparticle. Internal bonds are in red and boundary edges in blue. Edge pairs in the same direction is converted to a single super-edge.

Within each class, we integrate out the internal degrees of freedom—constituent identities and internal bonds—by performing a Boltzmann-weighted average over all microstates in the class to define a single canonical (effective) plaquette. The resulting free energy per lattice site for a mixture of plaquettes is then

$$\begin{aligned} \bar{f} &= \frac{1}{4} (f_{\text{entropy}} + f_{\text{association}} + f_{\text{intra-bonds}}) \\ &= \frac{1}{4} \sum_p \psi_p \left(\ln \frac{\psi_p}{g_p} + \sum_s m_p^s \left(\ln X_p^s - \frac{X_p^s}{2} + \frac{1}{2} \right) + \mu_p \right) \end{aligned} \quad (4)$$

where the factor of 4 accounts the number of sites in a plaquettes and ensures that f remains the free energy per site, ψ_p is the fraction of plaquette p and g_p accounts for rotational multiplicity/degeneracy of plaquette p . X_p^s is the unbounded fraction of type s superpatches on type p plaquette. The non-directional and directional bonds within plaquettes and the chemical potential of constituent monomers are captured by the last term. Specifically,

$$\begin{aligned} \mu_p &= \sum_{i=1}^4 \mu_i + \varepsilon_{12} + \varepsilon_{24} + \varepsilon_{13} + \varepsilon_{34}, \\ \varepsilon_{ij} &= \varepsilon_{ij,d} + \varepsilon_{ij,nd} \end{aligned} \quad (5)$$

where μ_i is the chemical potential of the monomer i and ε_{ij} is the total interaction coupling between monomer i and j including the directional (d) and non-directional (nd) terms.

Given n monomer species, we enumerate the distinct 2×2 plaquettes and obtain N unique plaquette classes after accounting for degeneracies. Let $\vec{\psi} \in \Delta^N$ denote the plaquette-fraction vector and $\vec{\phi} \in \Delta^n$ the monomer-fraction vector. The linear map $C : \Delta^N \rightarrow \Delta^n$ relates these compositions by counting the monomer constituents of each plaquette, i.e., $\vec{\phi} = C\vec{\psi}$. The monomer-level free-energy density is then obtained by contracting

the plaquette free energy,

$$f(\vec{\phi}) = \inf_{\vec{\psi} \in \Delta^N: C\vec{\psi}=\vec{\phi}} \bar{f}(\vec{\psi}), \quad (6)$$

which is the standard contraction of a higher-dimensional variational problem onto the monomer composition space [44–46]. In practice, this requires minimizing $f(\vec{\psi})$ over N plaquette fractions subject to the simplex constraints and the linear composition constraint $C\vec{\psi} = \vec{\phi}$. We perform this constrained optimization with a first-order method (AdaGrad), which is stable and scales to large N in our setting. The main practical limitation is scaling with chemical complexity: for n monomer species, the number of distinct 2×2 plaquettes grows as $O(n^4)$ (before symmetry reduction), increasing the contraction dimension accordingly.

Moving on to case studies, since topology matters already in pure solutions of single species, we first quantify its impact by generating patchy-solvent phase diagrams of two-patch particle with different patch organizations. We then turn to a few-component mixture where patch geometry induces an isomer-isomer separation.

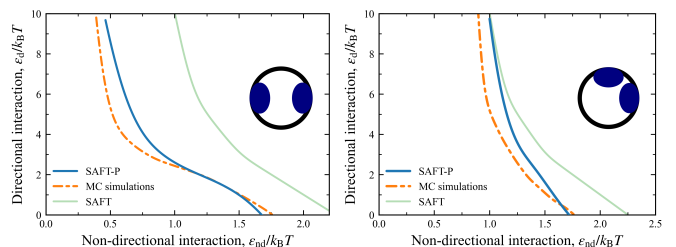


FIG. 2. Critical lines for stick-shaped (left) and L-shaped (right) particles as a function of directional and non-directional interaction strengths; insets depict the corresponding patch geometries.

Single-component patchy-particle solutions with identical patches are the simplest systems that still exhibit geometric (spatial) constraints. We study two-patch particles on a square lattice with either a 90° patch arrangement (L-shaped) or a 180° arrangement (stick-shaped). Patch-patch interactions are directional, while particle-particle interactions are non-directional and apply only between non-solvent particles. We performed grand-canonical (μVT) Monte Carlo simulations on a 10×10 square lattice using Metropolis sampling, with random identity change of patchy particles by defining each rotational degrees of freedom and empty sites as individual species without introducing any sampling bias. From simulations, we trace the critical line using mixed-field order parameters and tuning the chemical potentials for coexistence with histogram-reweighting techniques [35, 47], exploiting the mapping of binary lattice mixtures into the Ising universality class [48]. Within SAFT/SAFT-P, we locate the spinodal by the loss of convexity of the free

energy $f(\phi)$, i.e., when the smallest eigenvalue of the Hessian with respect to species densities vanishes. We then compute the binodal via a spinodal-seeded (spinodal-assisted) common-tangent construction, using the spinodal points as initial bracketing/initial guesses for the coexistence search.

Monte Carlo simulations provide a numerically exact route to equilibrium properties and are sufficient, in principle, to determine coexistence and criticality. In practice, however, producing an accurate phase diagram is substantially more costly and methodologically involved than a single equilibrium run: one must ensure equilibration across many state points, tune fields/chemical potentials to enforce coexistence, verify histogram overlap for reweighting, control finite-size effects, and account for critical slowing down near the critical region. The resulting workflow is implementation-heavy and can be opaque to reproduce, as outcomes depend on the specific choice of order parameters, biasing/reweighting strategy, and tuning protocol. By contrast, SAFT-P trades sampling for a deterministic free-energy construction: phase boundaries follow from convexity loss and common-tangent conditions, enabling systematic parameter sweeps without additional coexistence tuning or statistical noise.

In Fig. 2, we compile critical points across interaction settings and delineate the resulting critical line in the $(\epsilon_{\text{nd}}, \epsilon_{\text{d}})$ plane. Below this boundary the system remains single phase, whereas above it phase separation occurs for appropriate compositions and chemical potentials. Standard SAFT captures the critical line for L-shaped particles reasonably well but shows larger deviations for stick-shaped particles. We attribute this difference to particle geometry: L-shaped particles have greater rotational freedom and can form more isotropic, globular bonding networks, mitigating the impact of SAFT’s simplifying assumptions. In contrast, the stick geometry constrains bonding and promotes more anisotropic network growth, for which standard SAFT is less accurate. SAFT-P improves on standard SAFT by explicitly resolving the dominant local motif for sticks—stacked configurations within (2×2) plaquettes. As a result, SAFT-P not only reproduces the critical line for stick-shaped particles but also shows that the leading instability is driven by fluctuations in the population of stacked plaquettes, i.e., incipient aggregation of these stacked motifs.

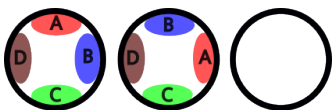


FIG. 3. Components of the proposed isomeric mixture, From right to left: geometric isomer 1, geometric isomer 2, solvent

Geometric isomers can exhibit distinct phase behavior in designed or spatially constrained environments. Cap-

turing this sensitivity requires a treatment beyond standard SAFT, because the free energy depends not only on composition but also on patch geometry and directional bonding patterns. Here we introduce a minimal ternary lattice model consisting of two geometric isomers and an inert solvent. The patch layouts of the two isomers and the solvent are shown in Fig. 3. We include directional attractions between complementary patch pairs A–C and B–D, together with like-like self attractions C–C and D–D, choosing $(\epsilon_{CC} = \epsilon_{DD} \equiv \epsilon_s)$ and $(\epsilon_{AC} = \epsilon_{BD} = 1.5\epsilon_s)$. This hierarchy favors the designed A–C/B–D bonds; consequently, an isolated isomer embedded in a region rich in the other isomer cannot simultaneously satisfy its preferred bonding pattern, creating local bonding frustration at the interface and within mixed domains.

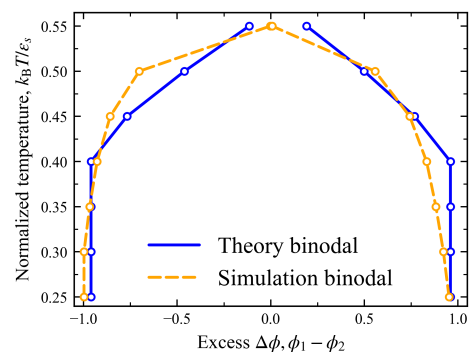


FIG. 4. Binodal of the isomeric mixture. Coexistence curve plotted as normalized temperature versus excess composition, where ϕ_1, ϕ_2 are the isomeric fractions in the two coexisting phases. Solid blue: theoretical binodal from plaquette coarse-grained free-energy / SAFT-P. Dashed orange: simulation binodal from Monte Carlo simulations on an 20×20 lattice

Because the solvent is noninteracting, changing its fraction mainly dilutes the mixture and does not qualitatively change the coexistence physics, aside from finite-size effects. We therefore fix the solvent fraction to $1/2$, which reduces the problem to a one-dimensional composition scan. On the theory side, we compute the SAFT-P free energy along this cut and obtain the binodal via a common-tangent construction. Monte Carlo simulations are performed in a mixed canonical–grand-canonical setup: the solvent is treated canonically (its number is fixed), while the two isomeric components are sampled grand canonically at fixed (zero) chemical potentials. In the two-phase regime the distribution of the isomeric excess becomes bimodal; we identify the peak locations and use them to construct the binodal from simulation.

Figure 4 compares the coexistence curve obtained from SAFT-P with Monte Carlo results. The two binodals show close agreement across the scanned compositions, and SAFT-P reproduces the critical temperature of the ternary mixture on this finite lattice. In contrast,

standard SAFT does not distinguish the two geometric isomers at fixed valence and interaction strengths and therefore cannot capture the excess-composition binodal. These results emphasize that incorporating plaquette-scale correlations resolves the geometry-induced bias in local bonding and its thermodynamic consequences in a minimal isomeric mixture.

We introduced SAFT-P, a plaquette-level extension of SAFT that retains local correlation and patch-topology information by treating 2×2 clusters as associating superparticles and contracting their free energy back to monomer densities. Across single- and few-component lattice mixtures, SAFT-P systematically improves phase-boundary predictions relative to standard SAFT: it captures the dominant stacked motif governing the instability of stick-shaped particles and correctly resolves geometric-isomer separation in a minimal ternary mixture where conventional SAFT remains topology-blind. More broadly, these results show that incorporating a small amount of local structure into an analytic associating-fluid framework can reconcile tractability with topology sensitivity, providing a route to model designed patchy mixtures and membrane-like two-dimensional condensates. Extensions to larger clusters, additional interaction motifs, and higher-component mixtures follow naturally within the same construction.

* hamzaco@mit.edu

† aalexand@mit.edu

- [1] S. F. Banani, H. O. Lee, A. A. Hyman, and M. K. Rosen, Biomolecular condensates: organizers of cellular biochemistry, *Nature reviews Molecular cell biology* **18**, 285 (2017).
- [2] Y. Shin and C. P. Brangwynne, Liquid phase condensation in cell physiology and disease, *Science* **357**, eaaf4382 (2017).
- [3] S. Alberti, A. Gladfelter, and T. Mittag, Considerations and challenges in studying liquid-liquid phase separation and biomolecular condensates, *Cell* **176**, 419 (2019).
- [4] E. Bianchi, R. Blaak, and C. N. Likos, Patchy colloids: state of the art and perspectives, *Physical Chemistry Chemical Physics* **13**, 6397 (2011).
- [5] Z. Zhang and S. C. Glotzer, Self-assembly of patchy particles, *Nano Letters* **4**, 1407 (2004).
- [6] P. Li, S. Banjade, H.-C. Cheng, S. Kim, B. Chen, L. Guo, M. Llaguno, J. V. Hollingsworth, D. S. King, S. F. Banani, *et al.*, Phase transitions in the assembly of multivalent signalling proteins, *Nature* **483**, 336 (2012).
- [7] X. Su, J. A. Ditlev, E. Hui, W. Xing, S. Banjade, J. Okrut, D. S. King, J. Taunton, M. K. Rosen, and R. D. Vale, Phase separation of signaling molecules promotes t cell receptor signal transduction, *Science* **352**, 595 (2016).
- [8] N. Dorsaz, L. Fillion, F. Smallenburg, and D. Frenkel, Spiers memorial lecture: Effect of interaction specificity on the phase behaviour of patchy particles, *Faraday Discussions* **159**, 9 (2012).
- [9] Y. Zhu, A. Bansal, S. Xi, J. Lu, and W. G. Chapman, Self-assembly and phase behavior of mixed patchy colloids with any bonding site geometry: theory and simulation, *Soft Matter* **16**, 3806 (2020).
- [10] D. J. Audus, F. W. Starr, and J. F. Douglas, Valence, loop formation and universality in self-assembling patchy particles, *Soft Matter* **14**, 1622 (2018).
- [11] H. Zhou, J. Hutchings, M. Shiozaki, X. Zhao, L. K. Doolittle, S. Yang, R. Yan, N. Jean, M. Riggi, Z. Yu, E. Villa, and M. K. Rosen, Quantitative spatial analysis of chromatin biomolecular condensates using cryoelectron tomography, *Proceedings of the National Academy of Sciences* **122**, e2426449122 (2025).
- [12] J. Russo, P. Tartaglia, and F. Sciortino, Association of limited valence patchy particles in two dimensions, *Soft Matter* **6**, 4229 (2010).
- [13] T. Litschel, C. F. Kelley, X. Cheng, L. Babl, N. Mizuno, L. B. Case, and P. Schwille, Membrane-induced 2d phase separation of the focal adhesion protein talin, *Nature Communications* **15**, 4986 (2024).
- [14] C.-P. Hsu, J. Aretz, A. Hordeichyk, R. Fassler, and A. R. Bausch, Surface-induced phase separation of reconstituted nascent integrin clusters on lipid membranes, *Proceedings of the National Academy of Sciences* **120**, e2301881120 (2023).
- [15] C.-W. Lin, L. M. Nocka, B. L. Stinger, J. B. DeGrandchamp, L. N. Lew, S. Alvarez, H. T. Phan, Y. Kondo, J. Kuriyan, and J. T. Groves, A two-component protein condensate of the egfr cytoplasmic tail and grb2 regulates ras activation by sos at the membrane, *Proceedings of the National Academy of Sciences* **119**, e2122531119 (2022).
- [16] L. B. Case, X. Zhang, J. A. Ditlev, and M. K. Rosen, Stoichiometry controls activity of phase-separated clusters of actin signaling proteins, *Science* **363**, 1093 (2019).
- [17] S. F. Shimobayashi, P. Ronceray, D. W. Sanders, M. P. Haataja, and C. P. Brangwynne, Nucleation landscape of biomolecular condensates, *Nature* **599**, 503 (2021).
- [18] K. L. Saar, D. Qian, L. L. Good, A. S. Morgunov, R. Collepardo-Guevara, R. B. Best, and T. P. Knowles, Theoretical and data-driven approaches for biomolecular condensates, *Chemical Reviews* **123**, 8988 (2023).
- [19] W. M. Jacobs, Theory and simulation of multiphase coexistence in biomolecular mixtures, *Journal of Chemical Theory and Computation* **19**, 3429 (2023).
- [20] S. Mao, D. Kuldinow, M. P. Haataja, and A. Košmrlj, Phase behavior and morphology of multicomponent liquid mixtures, *Soft Matter* **15**, 1297 (2019).
- [21] S. H. van Leuken, R. A. van Benthem, R. Tuinier, and M. Vis, Predicting multi-component phase equilibria of polymers using approximations to flory-huggins theory, *Macromolecular Theory and Simulations* **32**, 2300001 (2023).
- [22] D. Zwicker and L. Laan, Evolved interactions stabilize many coexisting phases in multicomponent liquids, *Proceedings of the National Academy of Sciences* **119**, e2201250119 (2022).
- [23] K. Shrinivas and M. P. Brenner, Phase separation in fluids with many interacting components, *Proceedings of the National Academy of Sciences* **118**, e2108551118 (2021).
- [24] J.-M. Choi, A. S. Holehouse, and R. V. Pappu, Physical principles underlying the complex biology of intracellular phase transitions, *Annual review of biophysics* **49**, 107 (2020).

- [25] T. S. Harmon, A. S. Holehouse, M. K. Rosen, and R. V. Pappu, Intrinsically disordered linkers determine the interplay between phase separation and gelation in multivalent proteins, *elife* **6**, e30294 (2017).
- [26] A. N. Semenov and M. Rubinstein, Thermoreversible gelation in solutions of associative polymers. 1. statics, *Macromolecules* **31**, 1373 (1998).
- [27] E. A. Müller and K. E. Gubbins, Molecular-based equations of state for associating fluids: A review of soft and related approaches, *Industrial & Engineering Chemistry Research* **40**, 2193 (2001).
- [28] P. Teixeira and J. Tavares, Phase behaviour of pure and mixed patchy colloids—theory and simulation, *Current opinion in colloid & interface science* **30**, 16 (2017).
- [29] D. W. Sanders, N. Kedersha, D. S. Lee, A. R. Strom, V. Drake, J. A. Riback, D. Bracha, J. M. Eeftens, A. Iwanicki, A. Wang, *et al.*, Competing protein-rna interaction networks control multiphase intracellular organization, *Cell* **181**, 306 (2020).
- [30] J. R. Espinosa, J. A. Joseph, I. Sanchez-Burgos, A. Garaizar, D. Frenkel, and R. Collepardo-Guevara, Liquid network connectivity regulates the stability and composition of biomolecular condensates with many components, *Proceedings of the National Academy of Sciences* **117**, 13238 (2020).
- [31] Y. Dai, L. You, and A. Chilkoti, Engineering synthetic biomolecular condensates, *Nature Reviews Bioengineering* **1**, 466 (2023).
- [32] K. P. Shukla and W. G. Chapman, Tpt2 and saftd equations of state for mixtures of hard chain copolymers, *Molecular Physics* **98**, 2045 (2000).
- [33] L. Vlček, J. Slovák, and I. Nezbeda, Thermodynamic perturbation theory of the second order: Implementation for models with double-bonded sites, *Molecular Physics* **101**, 2921 (2003).
- [34] I. G. Economou, Statistical associating fluid theory: A successful model for the calculation of thermodynamic and phase equilibrium properties of complex fluid mixtures, *Industrial & engineering chemistry research* **41**, 953 (2002).
- [35] W. M. Jacobs, D. W. Oxtoby, and D. Frenkel, Phase separation in solutions with specific and nonspecific interactions, *The Journal of Chemical Physics* **140**, 204112 (2014).
- [36] P. I. C. Teixeira and F. Sciortino, Patchy particles at a hard wall: Orientation-dependent bonding, *The Journal of Chemical Physics* **151**, 174903 (2019).
- [37] S. Shikha, P. Priyanka, and S. Maiti, Inversion of enzymatic enantioselectivity mediated by biomolecular condensates, *Biomacromolecules* **26**, 5096 (2025).
- [38] B. Pi-Boleda, S. Ramisetty, O. Illa, V. Branchadell, R. S. Dias, and R. M. Ortuno, Efficient dna condensation induced by chiral β -amino acid-based cationic surfactants, *ACS applied bio materials* **4**, 7034 (2021).
- [39] R. P. Sear and G. Jackson, Thermodynamic perturbation theory for association into chains and rings, *Phys. Rev. E* **50**, 386 (1994).
- [40] B. D. Marshall and W. G. Chapman, Thermodynamic perturbation theory for associating fluids with small bond angles: Effects of steric hindrance, ring formation, and double bonding, *Phys. Rev. E* **87**, 052307 (2013).
- [41] M. S. Wertheim, Fluids with highly directional attractive forces. ii. thermodynamic perturbation theory and integral equations, *Journal of Statistical Physics* **35**, 35 (1984).
- [42] W. Zmpitas and J. Gross, Detailed pedagogical review and analysis of wertheim’s thermodynamic perturbation theory, *Fluid Phase Equilibria* **428**, 121 (2016).
- [43] N. G. Almarza, J. M. Tavares, E. G. Noya, and M. Telo da Gama, Three-dimensional patchy lattice model for empty fluids, *The Journal of Chemical Physics* **137**, 244902 (2012).
- [44] H. Touchette, The large deviation approach to statistical mechanics, *Physics Reports* **478**, 1 (2009).
- [45] S. S. Varadhan, Large deviations, in *Proceedings of the International Congress of Mathematicians 2010 (ICM 2010) (In 4 Volumes) Vol. I: Plenary Lectures and Ceremonies Vols. II–IV: Invited Lectures* (World Scientific, 2010) pp. 622–639.
- [46] R. S. Ellis, *Entropy, large deviations, and statistical mechanics*, Vol. 271 (Springer Science & Business Media, 2012).
- [47] A. M. Ferrenberg and R. H. Swendsen, New monte carlo technique for studying phase transitions, *Phys. Rev. Lett.* **61**, 2635 (1988).
- [48] N. Wilding, Critical point field mixing in an asymmetric lattice gas model, *Zeitschrift für Physik B Condensed Matter* **93**, 119 (1993).